available at www.sciencedirect.com

SCIENCE DIRECT®

journal homepage: www.elsevier.com/locate/biochempharm

Generation of adenosine A_3 receptor functionally humanized mice for the evaluation of the human antagonists

Kazuya Yamano [a], *Miho Inoue* [a], *Shigehiro Masaki* [b], *Mayumi Saki* [b], *Michio Ichimura* [a], *Mitsuo Satoh* [a,*]

[a] *Tokyo Research Laboratories, Kyowa Hakko Kogyo Co. Ltd., 3-6-6 Asahi-machi, Machida-shi, Tokyo 194-8533, Japan*
[b] *Pharmaceutical Research Center, Kyowa Hakko Kogyo Co. Ltd., 1188 Shimotogari, Nagaizumi-cho, Sunto-gun, Shizuoka 411-8731, Japan*

ARTICLE INFO

Article history:
Received 2 September 2005
Accepted 17 October 2005

Keywords:
Adenosine A3 receptor
G protein-coupled receptor
Chimeric receptor
Uncoupling
A3AR functionally humanized mice
Species difference

Abbreviations:
A3AR, adenosine A3 receptor
$A3AR^{c/c}$ mice,
A3AR-chimeric mice
$A3AR^{h/h}$ mice,
A3AR-humanized mice
BMMCs, bone marrow-derived mast cells
$[Ca^{2+}]_i$, intracellular Ca^{2+} concentration
Cl-IB-MECA, 2-chloro-N^6-(3-iodobenzyl)adenosine-5′-N-methyluronamide
DT-A, diphtheria toxin A fragment

ABSTRACT

Although the adenosine A_3 receptor (A3AR), which is a $G_{i/o}$ protein-coupled receptor, has attracted considerable interest as a potential target for drugs against asthma or inflammation, the in vivo evaluation of the antagonists using rodents in the first step of drug development has been hampered by the lack of highly potent antagonists for the rodent A3AR. To evaluate the pharmacological effects of human A3AR antagonists in mice, we previously generated A3AR-humanized mice, in which the mouse A3AR gene was replaced by its human counterpart. However, the human A3AR did not lead to the phosphoinositide 3-kinase (PI3K) γ-signaling pathway such as IgE/antigen-dependent mast cell degranulation, probably due to the uncoupling of the mouse $G_{i/o}$ protein(s). To overcome the uncoupling, we here generated A3AR functionally humanized mice by replacing the mouse A3AR gene with a human/mouse chimeric A3AR sequence in which whole intracellular regions of the human A3AR were substituted for the corresponding regions of the mouse A3AR. The chimeric A3AR led to intracellular Ca^{2+} elevation and activation of the PI3Kγ-signaling pathway, which are equivalent to the actions induced by A3AR in wild-type mice. The human A3AR antagonist had the same binding affinities for the chimeric A3AR as the human A3AR and completely antagonized this potentiation. This is the first direct evidence that the uncoupling of mouse G protein(s) to the human A3AR is due to a sequence difference in the intracellular regions of A3AR. The A3AR functionally humanized mice can be widely employed for pharmacological evaluations of the human A3AR antagonists.

* *Corresponding author*. Tel.: +81 42 725 2555; fax: +81 42 726 8330.
E-mail address: msatoh@kyowa.co.jp (M. Satoh).
0006-2952/$ – see front matter
doi:10.1016/j.bcp.2005.10.028

ERK1/2, extracellular signal-regulated kinase 1/2
ES cells, embryonic stem cells
GPCR, G protein-coupled receptor
HAT, hypoxanthine/aminopterin/thymidine
HPRT, hypoxanthine phosphoribosyltransferase
[^{125}I]AB-MECA, N^6-(4-amino-3-[^{125}I]iodobenzyl)adenosine-5′-N-methyluronamide
KF26777, 2-(4-bromophenyl)-7,8dihydro-4-propyl-1*H*-imidazo[2,1-i]purin-5(4*H*)-one dihydrochloride
MAPK, mitogen-activated protein kinase
PCR, polymerase chain reaction
PI3Kγ, phosphoinositide 3-kinase γ
PKB, protein kinase B
(*R*)-PIA, (R)-N^6-phenylisopropyladenosine
RT-PCR, reverse transcription-PCR
TNP, 2,4,6-trinitrophenyl
anti-TNP IgE, monoclonal IgE antibody against 2,4,6-trinitrophenyl

1. Introduction

G protein-coupled receptors (GPCRs) play key roles in diverse cellular processes, and these receptors are also known as attractive targets of therapeutic agents against various human diseases [1–4]. The GPCRs are the target of over 50% of the modern therapeutic agents on the market, and large numbers of novel compounds for GPCRs are continuously being identified and developed [3]. In this process of drug discovery and development, animal studies using rodents are important steps for understanding the in vivo physiological roles of the target GPCRs and evaluating the pharmacological effects of the agents against the target diseases. However, the in vivo studies for the human-selective agents are often hampered severely by the low affinities for the rodent GPCRs, due to the low homology between the human and rodent GPCRs [5]. This is particularly true for adenosine A_3 receptor (A3AR), which shows only 74% homology between humans and rodents (other GPCRs usually show sequence homologies ranging from 85 to 95% between different species) [6,7].

The A3AR is one of the four GPCRs for adenosine; it is expressed in a broad spectrum of tissues and couples to $G_{i/o}$ proteins [8–10]. The ligand-stimulated A3AR leads to the elevation of intracellular Ca^{2+} concentration ($[Ca^{2+}]_i$) and the activation of phosphoinositide 3-kinase (PI3K) γ [11,12]. The activated PI3Kγ leads to the phosphorylation of protein kinase B (PKB) and members of the mitogen-activated protein kinase (MAPK) family, including extracellular signal-regulated kinase (ERK) 1/2 and p38 [11,13]. This A3AR-stimulated PI3Kγ-dependent signaling pathway is essential for the potentiation of IgE/antigen-dependent mast cell degranulation [14] and the A3AR internalization [15].

Many studies have reported that the A3AR plays a role in a diverse range of diseases [7,16] by regulating apoptotic cell death and the cell cycle [17–19] and by activating mast cells [14,20–24], eosinophils [25,26], neutrophils [27], and natural killer cells [28]. These reports suggest that the A3AR-selective agents might be therapeutically useful for treatment of human diseases. Indeed, recent studies using mast cell lines and A3AR-deficient mice have shown that the A3AR antagonists have potential as anti-asthmatic and anti-inflammatory drugs [6,7,16,21–23,26]. Highly potent and selective antagonists for the human A3AR have been screened and identified (K_i values in the 0.1 nM range) [6,7]. However, all of the A3AR antagonists have 1000 times lower affinities for the rodent A3AR (K_i values in the 0.1 μM range) than for the human A3AR, because of the low interspecies homology between the human and rodent A3AR [6,7]. The lack of highly potent antagonists for the rodent A3AR makes it very difficult to evaluate the pharmacological potency of the A3AR antagonists in treatment for these diseases in rodent models.

In our previous study, we generated A3AR-humanized mice ($A3AR^{h/h}$ mice), in which the A3AR gene was replaced by its human counterpart, in order to evaluate pharmacological effects of the human A3AR antagonists in mice [29]. The human A3AR normally led to the mobilization of $[Ca^{2+}]_i$ in $A3AR^{h/h}$ mice. However, unexpectedly, the human A3AR did not lead to the phosphorylation of PKB and ERK1/2, the

potentiation of IgE/antigen-dependent mast cell degranulation, or the A3AR internalization in $A3AR^{h/h}$ mice, probably due to the uncoupling of member(s) of the mouse G proteins for the activation of PI3Kγ. Although KF26777, a highly potent and selective antagonist for the human A3AR [30], bound to the human A3AR (K_i value, 0.2 nM) and completely antagonized the $[Ca^{2+}]_i$ elevation in $A3AR^{h/h}$ mice, the pharmacological effects of KF26777 as an anti-inflammatory agent could not be evaluated because the mast cell degranulation was not potentiated.

To overcome the uncoupling, we here generated A3AR functionally humanized mice ($A3AR^{c/c}$ mice) by replacing the mouse A3AR gene with a human/mouse chimeric A3AR sequence in which whole intracellular regions of the human A3AR were substituted for the corresponding regions of the mouse A3AR. In $A3AR^{c/c}$ mice, the chimeric A3AR led to intracellular Ca^{2+} elevation and activation of the PI3Kγ-signaling pathway, including such actions as the phosphorylation of ERK1/2 and PKB, the potentiation of IgE/antigen-dependent mast cell degranulation, and the A3AR internalization, all of which are equivalent to those induced by A3AR in wild-type mice. The human A3AR antagonist had the same binding affinities for the chimeric A3AR as the human A3AR and completely antagonized this potentiation. These results demonstrate that A3AR functionally humanized mice can be widely employed for pharmacological evaluations of the human A3AR antagonists. This is the first direct evidence that the uncoupling of mouse G protein(s) to the human GPCR A3AR is due to the sequence difference in intracellular regions of the receptor, and should provide new insight into the mechanism of G protein/GPCR coupling and its differences among species.

2. Materials and methods

2.1. Animals

C57BL/6J mice, which were used as wild-type control, were purchased from CLEA Japan (Tokyo, Japan). The human A3AR-humanized mice ($A3AR^{h/h}$ mice) were generated and genotyped as previously described [29]. All animals were maintained under a specific pathogen-free condition. This study was conducted according to the Guidelines for the Care and Use of Laboratory Animals of Kyowa Hakko Kogyo Co. Ltd., in compliance with national laws and policies.

2.2. Materials

N^6-(4-Amino-3-[^{125}I]iodobenzyl)adenosine-5′-*N*-methyluronamide ([^{125}I]AB-MECA, specific activity, 74 TBq/mmol) was purchased from Amersham (Buckinghamshire, UK). Adenosine deaminase and (*R*)-N^6-phenylisopropyladenosine ((*R*)-PIA) were from Sigma (St. Louis, MO). Rabbit anti-ERK1/2 antibody, rabbit anti-phospho ERK1/2 (Thr202/Tyr204) antibody, rabbit anti-PKB antibody, rabbit anti-phospho PKB (Ser473) antibody, and the Phototope-HRP Western Blot Detection Kit were from Cell Signals Technology (Beverly, MA). Fluo-3 AM and Fula-2 AM was from Molecular Probes (Eugene, OR). 2-Chloro-N^6-(3-iodobenzyl)adenosine-5′-*N*-methyluronamide (Cl-IB-MECA) and 2-(4-bromophenyl)-7,8dihydro-4-propyl-1*H*-imidazo[2,1-i]purin-5(4*H*)-one dihydrochloride (KF26777) were synthesized in our laboratories. 2,4,6-Trinitrophenyl bovine serum albumin (TNP-BSA) was from LSL (Tokyo, Japan). Mouse monoclonal IgE antibody against 2,4,6-trinitrophenyl (anti-TNP IgE) was purified from the culture supernatants of a TNP-immunized mouse B lymphocyte cell line (American Type Culture Collection number; TIB-142).

2.3. Construction of a targeting vector for chimeric A3AR mice

The chimeric A3AR sequence (shown in Fig. 2B) was synthesized by polymerase chain reaction (PCR) with overlapping oligonucleotides according to the method described previously [31]. The targeting vector designed to replace the open reading frame of the mouse A3AR gene by the chimeric A3AR sequence was constructed by replacing the human A3AR cDNA sequence with the chimeric A3AR sequence in the targeting vector for $A3AR^{h/h}$ mice [29]. Briefly, the targeting vector consists of the diphtheria toxin A fragment (DT-A) expression cassette as a negative selectable marker, a 6-kb mouse genomic DNA region (from the *Sma* I site in the 5′ external sequence to immediately upstream of the *ATG* initiation codon in exon 1 of the A3AR gene), the chimeric A3AR sequence, a 0.45-kb mouse genomic DNA region (from immediately downstream of the *TAG* stop codon to the polyadenylation site in exon 2 of the A3AR gene), the *lox*P site-flanked hypoxanthine phosphoribosyltransferase (HPRT) expression cassette as a positive selectable marker, and a 2.8-kb mouse genomic DNA region (from the *Bam*H I site in exon 2 to the *Apa* I site in the 3′ external sequence) (Fig. 3A).

2.4. Homologous recombination in ES cells

The *Sal* I-linearized targeting vector was electroporated into mouse embryonic stem (ES) cell line AB2.2 from the 129/SvEv strain (Lexicon, The Woodlands, TX). Selected clones for resistance to hypoxanthine/aminopterin/thymidine (HAT) selection medium (Lexicon) were verified by Southern blot analysis using two external probes derived from the 5′ external sequence from the *Eco*R I site to the *Sma* I site and the 3′ external sequence from the *Apa* I site to the *Eco*R I site (Fig. 3A). Identified homologous recombinant clones were transiently transfected with Cre recombinase expression vector pBS185 (Invitrogen, Carlsbad, CA) for the removal of the HPRT expression cassette from the recombinant allele. Clones were screened in 6-thioguanine (Sigma) and the deletion of the HPRT cassette was verified by Southern blot analysis using the external probes.

2.5. Generation of $A3AR^{c/c}$ mice

The ES cell clones were injected into 3.5-day-old blastocysts from C57BL/6J mice (CLEA, Japan) and were transferred into the oviducts of pseudopregnant ICR females (CLEA, Japan). The chimeric males were backcrossed to C57/BL6J mice and germ-line transmission of the recombinant allele was detected by Southern blot analysis of tail-biopsy DNA from agouti offspring using the 5′ or 3′ external probes. Heterozygotes were intercrossed to produce homozygotes and their

offspring were genotyped by Southern blot analysis using the 3′ external probe (Fig. 3B).

2.6. Generation of BMMCs

Bone marrow-derived mast cells (BMMCs) were generated from the femoral bone marrow cells of 8- to 10-week-old wild-type, $A3AR^{h/h}$, and $A3AR^{c/c}$ mice according to the method described previously [29]. Briefly, the cells were grown in BMMC medium consisting of RPMI 1640 (Invitrogen) supplemented with 10% (v/v) heat-inactivated fetal bovine serum (JRH Biosciences, Lenexa, KS), 50 μM 2-mercaptoethanol (Invitrogen), 10 mg/L gentamicin (Nacalai Tesque, Kyoto, Japan), 100 μM non-essential amino acids (Invitrogen), 100 μM sodium pyruvate (Invitrogen), and 10% (v/v) pokeweed mitogen-stimulated spleen-conditioned medium at 37 °C in a humidified atmosphere of 5% CO_2 in air. After 5 weeks, more than 95% of the nonadherent cells were identifiable as BMMCs, as determined by FACS analysis of the cell surface expression of c-kit and high-affinity IgE receptor.

2.7. Reverse transcription (RT)-PCR analysis

Total RNAs were isolated from mouse tissues and BMMCs using an RNeasy kit (QIAGEN, Hilden, Germany) and incubated for 1 h at 37 °C with 20 units of RNase-free DNase (Promega, Madison, WI) to degrade genomic DNA. After DNA digestion, the total RNAs were purified again using an RNeasy kit. The single-strand cDNAs were synthesized from 3 μg of each total RNA using a Superscript first-strand synthesis system for RT-PCR (Invitrogen). The two-fold diluted reaction mixtures were used as templates for the following PCR. The PCR was carried out by heating at 94 °C for 5 min, followed by 22 cycles (for β-actin) or 30 cycles (for A3ARs) of 94 °C for 1 min and 68 °C for 2 min in 20 μl of reaction mixture containing 1 μl of the two-fold diluted single-strand cDNA, 10 pmol of primers, 4 nmol of dNTP mixture, and ExTaq polymerase (TaKaRa BIO, Shiga, Japan) using a GeneAmp PCR System 9700 (Perkin-Elmer, Norwalk, CT). A 913-bp fragment of chimeric A3AR cDNA was amplified using primers 5′-AACAGCACTGCTCTGTCATTGGCC-3′ (designed as a sense primer to specifically anneal to the 1st extracellular region of human A3AR cDNA) and 5′-AATCTGAGGTCTGACAGAGCCT-GAG-3′ (designed as a antisense primer to specifically anneal to the 4th intracellular region of mouse A3AR cDNA), a 913-bp fragment of mouse A3AR cDNA was amplified using primers 5′-AACACCACGGAGACGGACTGGCTG-3′ (designed as a sense primer to specifically anneal to the 1st extracellular region of mouse A3AR cDNA) and 5′-AATCTGAGGTCTGACAGAGCCT-GAG-3′ (designed as a antisense primer to specifically anneal to the 4th intracellular region of mouse A3AR cDNA), and a 793-bp fragment of β-actin cDNA was amplified using primers 5′-GATATCGCTGCGCTCGTCGTCGAC-3′ and 5′-CAGGAAGGAA-GGCTGGAAGAGAGC-3′. The PCR products were subjected to electrophoresis in 1.2% agarose gel for analysis.

2.8. Receptor binding assay

The saturation binding assay with the A3AR agonist [^{125}I]AB-MECA was carried out according to a previous study [29]. Briefly, membranes of BMMCs (100 μg) were incubated for 120 min at 25 °C with 2 U/ml adenosine deaminase and 0.0625, 0.125, 0.25, 0.5, 1.0, or 2.0 nM [^{125}I]AB-MECA in a binding-assay buffer (50 mM Tris–HCl buffer, pH 7.4, containing 10 mM $MgCl_2$). The assays were performed in the presence of 1% of the final concentration of dimethyl sulfoxide and non-specific binding was determined in the presence of 100 μM (R)-PIA. After incubation, the binding reactions were terminated by filtration of the membranes through MultiScreen GF/B filter (Millipore, Bedford, MA). The filters were washed with ice-cold binding assay buffer, and the radioactivity was determined by COBRA γ-counter (Packard, Downers Grove, IL). The competitive binding assays were carried out according to the method described above (with the addition of 0.8 nM [^{125}I]AB-MECA and 0.001, 0.01, 0.1, 1.0, 10, or 100 nM KF26777).

2.9. Measurement of intracellular Ca^{2+} concentration

The measurement of $[Ca^{2+}]_i$ was carried out according to a previous study [29]. Briefly, BMMCs were incubated in BMMC medium with saturating concentrations of anti-TNP IgE (100 ng/ml/10^6 cells) overnight and were incubated for 60 min at 37 °C with 5 μM Fluo-3 AM or Fula-2 AM and 0.5% pluronic F-127 in the Ca^{2+} assay buffer (115 mM NaCl, 5.4 mM KCl, 0.8 mM $MgCl_2$, 1.8 mM $CaCl_2$, 13.8 mM glucose, 2.5 mM Probenecid, and 20 mM HEPES, pH 7.4, and 0.2% (w/v) BSA). After washing twice in Ca^{2+} assay buffer, the 2.5×10^4 cells were transferred to each well of 96-well plates and incubated for 20 min. The fluorescence intensity of Fluo-3 by the addition of 100 nM Cl-IB-MECA was quantified using FDSS 6000 (Hamamatsu Photonics, Shizuoka, Japan). The Fluo-3 intensities were monitored every second and were plotted as a ratio against the Fluo-3 intensity at the resting calcium level. The measurement of $[Ca^{2+}]_i$ mobilization using Fula-2 was carried out as followings. The 5.0×10^5 cells loaded with Fura-2 were transferred to each tubel and incubated for 30 min. The fluorescence intensity of Fura-2 by the addition of 100 nM Cl-IB-MECA was quantified using CAF-110 (Japan Spectroscopic, Tokyo, Japan). The Fura-2 intensities were monitored every second and were plotted as the fluorescence ratio at 340 and 380 nm. The data presented are representative of five independent experiments. For measurements of the antagonist activity, the BMMCs were pre-incubated with 100 nM KF26777 for 5 min (Fluo-3) or 2 min (Fura-2) prior to addition of 100 nM Cl-IB-MECA.

2.10. Western blot analysis

The phosphorylation of PKB and ERK1/2 induced by the A3AR was detected by the methods described previously [29]. Briefly, BMMCs stimulated by 1 μM Cl-IB-MECA at 37 °C for 0, 3, or 15 min were lysed in ice-cold lysis buffer (62.5 mM Tris–HCl, pH 6.8, 2% (w/v) SDS, 10% (v/v) glycerol, 50 mM dithiothreitol, 0.1% (w/v) bromophenol blue) and boiled for 2 min. The boiled samples were resolved by SDS-polyacrylamide gel electrophoresis using e-PAGEL 5–20% (w/v) polyacrylamide gels (ATTO, Tokyo, Japan). After transfer of the proteins onto polyvinylidene difluoride membranes, the protein phosphorylation was detected with rabbit phospho-specific ERK1/2 and phospho-specific PKB antibody using goat anti-rabbit horseradish peroxidase-coupled secondary antibody and a Phototope HRP Western Blot Detection Kit. To confirm equal loading

in each lane, parallel immunoblots were run in order to detect the unphosphorylated ERK1/2 and PKB.

2.11. *Internalization assay*

A3AR internalization was quantified by the changing rate of the receptor surface density after treatment of Cl-IB-MECA according to the methods described previously [29]. Briefly, after the stimulation of 1 μM Cl-IB-MECA for 15 min at 37 °C, the cells were washed twice with ice-cold PBS and the amounts of A3AR on the cell surface were evaluated as described above by *Receptor binding assay* (with the addition of 2 nM [^{125}I]AB-MECA. The A3AR density was expressed as the percentage of total binding versus control Cl-IB-MECA-untreated cells (100%).

2.12. *β-Hexosaminidase release assay*

β-Hexosaminidase release from BMMCs was measured by the methods described previously [29]. Briefly, 5×10^5 cells of anti-TNP IgE-saturated BMMCs were pre-incubated in the presence or absence of 10 nM KF26777 for 1 min prior to incubation with the indicated concentration of Cl-IB-MECA for 1 min at 37 °C in Tyrode buffer (130 mM NaCl, 5 mM KCl, 0.6 mM KH_2PO_4, 0.6 mM $MgCl_2$, 1 mM $CaCl_2$, 0.1% (w/v) glucose, 10 mM HEPES, pH 7.4, and 0.1% (w/v) BSA). The cells were stimulated with 10 ng/ml TNP-BSA for 30 min at 37 °C, and the amount of β-hexosaminidase released from BMMCs in the supernatant was measured as the β-hexosaminidase activity using *p*-nitrophenyl-*N*-acetyl-β-D-glucosaminide. The results were expressed as a percentage of the total TritonX-100-releasable β-hexosaminidase in whole cells.

2.13. *Data analysis*

The binding parameters were calculated using Prism software (GraphPAD, San Diego, CA). The IC_{50} values obtained from the competition curves were converted to K_i values by using the Cheng and Prusoff equation [32].

3. Results

3.1. *Targeted replacement of the mouse A3AR gene by the chimeric A3AR cDNA in mice*

We previously reported that the human A3AR can normally lead to the mobilization of $[Ca^{2+}]_i$ but is unable to potentiate

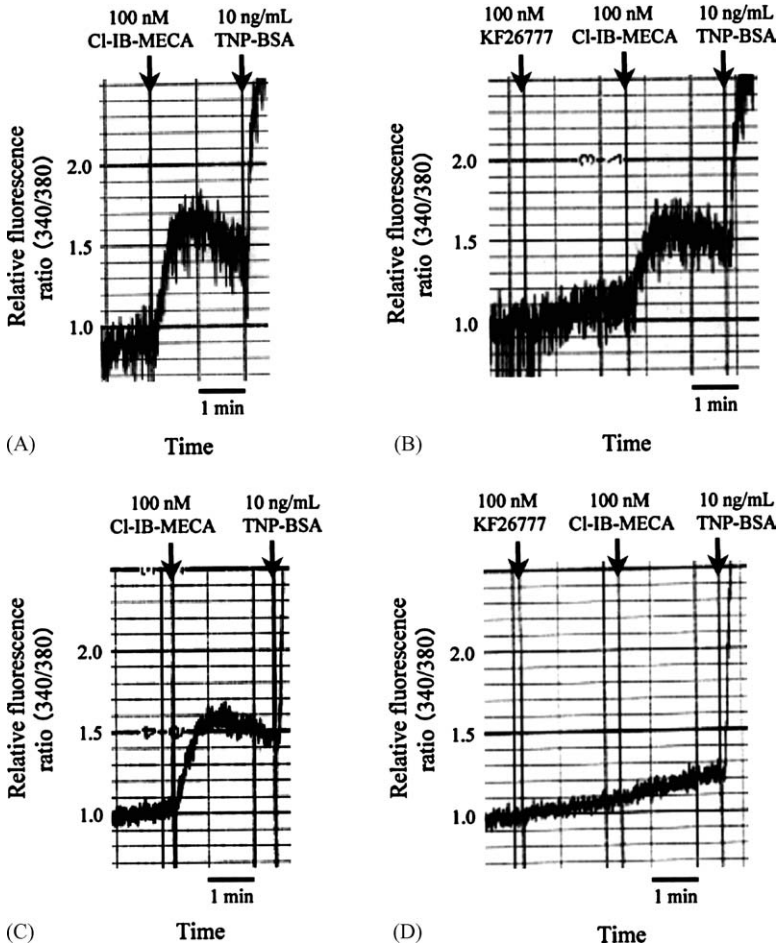

Fig. 1 – The human A3AR leads to the mobilization of $[Ca^{2+}]_i$ in mice. BMMCs derived from wild-type (A and B) and A3AR$^{h/h}$ mice (C and D) were preloaded with Fura-2 AM and then were stimulated with 100 nM Cl-IB-MECA in the absence (A and C) or presence (B and D) of 100 nM KF26777. The $[Ca^{2+}]_i$ mobilization by the addition of TNP-BSA via IgE receptor were measured as positive control. The Fura-2 intensities were plotted as the fluorescence ratio at 340 and 380 nm.

the mast cell degranulation in mice, probably due to the uncoupling of some mouse $G_{i/o}$ protein(s) to the human A3AR [29]. In this study, we first confirmed the human A3AR-induced $[Ca^{2+}]_i$ mobilization (Fig. 1) without potentiation of the mast cell degranulation by the human A3AR (as described below) in $A3AR^{h/h}$ mice. To overcome the uncoupling and evaluate highly potent and selective antagonists for the human A3AR in rodent models, we designed the human/mouse chimeric A3AR sequence, in which whole intracellular loop regions of the human A3AR were substituted for the equivalent regions of the mouse A3AR (Fig. 2). The replacement of the mouse A3AR gene by the chimeric A3AR sequence was carried out in mouse ES cells using a homologous recombination system according to the strategy

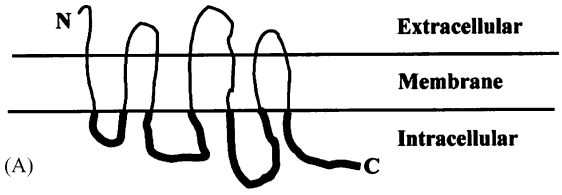

(A)

```
        10        20        30        40        50        60
atgcccaacaacagcactgctctgtcattggccaatgttacctacatcaccatggaaatt
M  P  N  N  S  T  A  L  S  L  A  N  V  T  Y  I  T  M  E  I

        70        80        90       100       110       120
ttcattggactctgcgccatagtgggcaacgtgctggtcatctgcgtggtcaagctgaac
F  I  G  L  C  A  I  V  G  N  V  L  V  I  C  V  V  K  L  N

       130       140       150       160       170       180
cccactctgcgtacgaccacctttctatttcattgtctctctagccctggctgacattgct
P  T  L  R  T  T  T  F  Y  F  I  V  S  L  A  L  A  D  I  A

       190       200       210       220       230       240
gttggggtgctggtcatgcctttggccattgttgtcagcctgggcatcacaatccacttc
V  G  V  L  V  M  P  L  A  I  V  V  S  L  G  I  T  I  H  F

       250       260       270       280       290       300
tacagctgccttttatgacttgcctactgcttatctttacccacgcctccatcatgtcc
Y  S  C  L  F  M  T  C  L  L  L  I  F  T  H  A  S  I  M  S

       310       320       330       340       350       360
ttgctggccatcgctgtggaccgatacttgcgggtcaagcttaccgtcagatacagaacg
L  L  A  I  A  V  D  R  Y  L  R  V  K  L  T  V  R  Y  R  T

       370       380       390       400       410       420
gtcaccactcaacgaaggatctggctggccctgggcctttgctggctggtgtcattcctg
V  T  T  Q  R  R  I  W  L  A  L  G  L  C  W  L  V  S  F  L

       430       440       450       460       470       480
gtgggattgacccccatgtttggctggaacatgaaactgacctcagagtaccacagaaat
V  G  L  T  P  M  F  G  W  N  M  K  L  T  S  E  Y  H  R  N

       490       500       510       520       530       540
gtcaccttcctttcatgccaatttgtttccgtcatgagaatggactacatggtatacttc
V  T  F  L  S  C  Q  F  V  S  V  M  R  M  D  Y  M  V  Y  F

       550       560       570       580       590       600
agcttcctcacctggattttcatccctctagttgtcatgtgtgccatctacctagacatc
S  F  L  T  W  I  F  I  P  L  V  V  M  C  A  I  Y  L  D  I

       610       620       630       640       650       660
ttctacatcatccgaaataagctcagtcaaaacctgtctggcttcagagagacgcgtgca
F  Y  I  I  R  N  K  L  S  Q  N  L  S  G  F  R  E  T  R  A

       670       680       690       700       710       720
ttttatggacgggaattcaagacggctaagtccttgtttctggttctttttcttgtttgct
F  Y  G  R  E  F  K  T  A  K  S  L  F  L  V  L  F  L  F  A

       730       740       750       760       770       780
ctgtcatggctgcctttatctatcatcaactgcatcatctactttaatggtgaggtacca
L  S  W  L  P  L  S  I  I  N  C  I  I  Y  F  N  G  E  V  P

       790       800       810       820       830       840
cagcttgtgctgtacatgggcatcctgctgtcccatgccaactccatgatgaaccctatc
Q  L  V  L  Y  M  G  I  L  L  S  H  A  N  S  M  M  N  P  I

       850       860       870       880       890       900
gtctacgcgtataaaataaaaaagttcaaagagacctactttctgatcctcagagctctc
V  Y  A  Y  K  I  K  K  F  K  E  T  Y  F  L  I  L  R  A  L

       910       920       930       940       950       960
aggctctgtcagacctcagattctttggactcaaacatggaacagactactgagtaa
R  L  C  Q  T  S  D  S  L  D  S  N  M  E  Q  T  T  E  stop
```

(B)

Fig. 2 – The design of human/mouse chimeric A3AR. (A) Schematic drawing of the putative secondary structure of the chimeric A3AR. The intracellular regions of the human A3AR were substituted for the corresponding regions of the mouse A3AR (thick lines). (B) The nucleotide and amino acid sequences of the chimeric A3AR. The sequences derived from the mouse A3AR are indicated by lines.

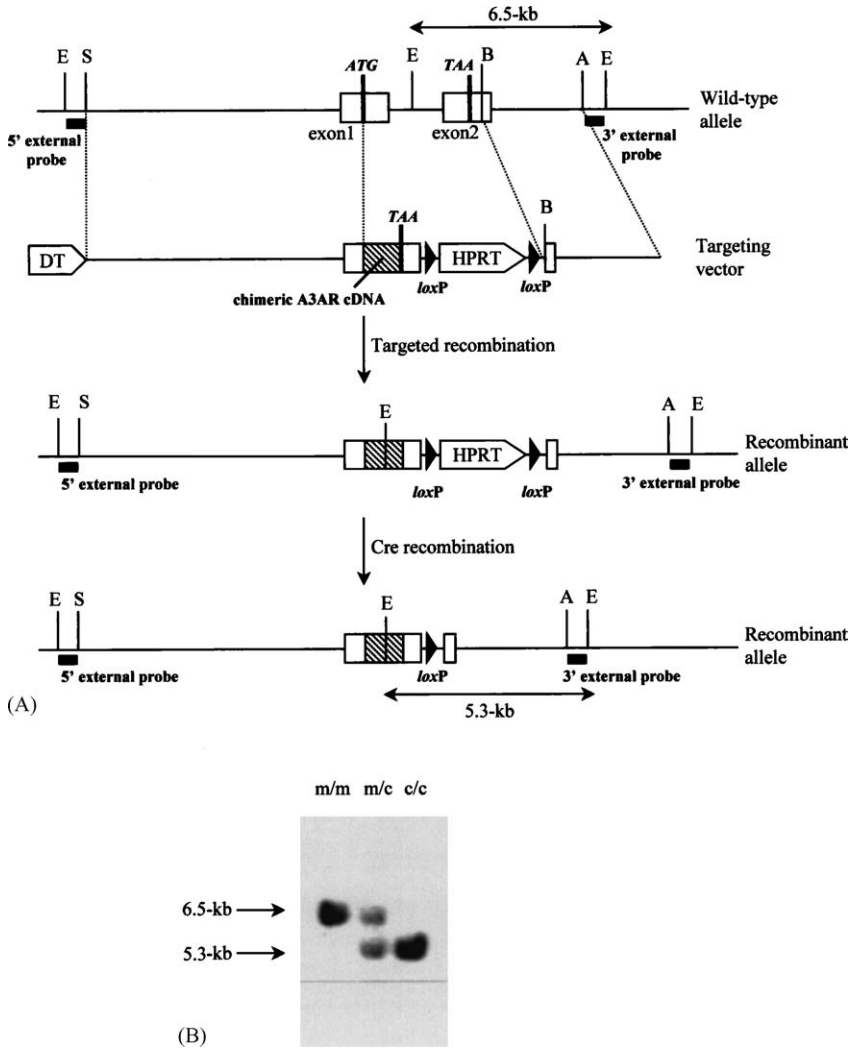

Fig. 3 – Targeted replacement of the mouse A3AR gene by the chimeric A3AR sequence. (A) Schematic drawing of the targeting vector and the recombinant alleles. Restriction sites *Apa* I (A), *Eco*R I (E), *Bam*H I (B), *Sma* I (S), and the location of the probe used for ES cell screening (two external probes derived from the 5′ external sequence from the *Eco*R I site to the *Sma* I site, and the 3′ external sequence from the *Apa* I site to the *Eco*R I site) and genotyping are indicated. The two exons are represented by open rectangles. The targeting vector contained a DT-A expression cassette as a negative selectable marker and an HPRT expression cassette as a positive selectable marker, and this vector replaced the region (from the *ATG* initiation codon to the *TAA* stop codon in the mouse A3AR gene) with the chimeric A3AR sequence (striped box) by homologous recombination. The HPRT expression cassette was removed from the genomic DNA by a Cre/*lox*P recombination system. (B) Genomic Southern analysis of A3AR$^{c/c}$ mice. After *Eco*R I digestion of genomic DNA purified from wild-type mice (m/m), A3AR$^{c/c}$ mice (c/c), and heterozygotes (m/c), the 3′ external-probe detected a 6.5-kb band in the wild-type allele and a 5.3-kb band in the targeted allele.

shown in Fig. 3A. After electroporation of the linearized targeting vector into the mouse ES cells, HAT-resistant clones were screened by Southern blot analysis. Eighteen of the 288 HAT-resistant clones had bands of the expected size for the targeted allele. Four of the 18 clones having the recombinant allele transiently expressed Cre recombinase, and removal of the HPRT expression cassette from the recombinant allele by the Cre/*lox*P recombination system in 6-thioguanine-resistant clones was confirmed by Southern blot analysis. Injection of the HPRT expression cassette-deleted clones into C57BL/6J blastocysts produced 15 chimeric males exhibiting contributions from the ES cells ranging from 50–100% as based on the amount of agouti coloring in the animal's coat. Six of these mice transmitted the recombinant allele through the germ line. The male chimeras were bred to C57BL/6J mice and heterozygous offspring (A3AR$^{m/c}$ mice) were born. Homozygous mice (A3AR$^{c/c}$ mice) were obtained in crosses between A3AR$^{m/c}$ mice. The phenotypes were detected by Southern blot analysis of DNA obtained by tail biopsy (Fig. 3B).

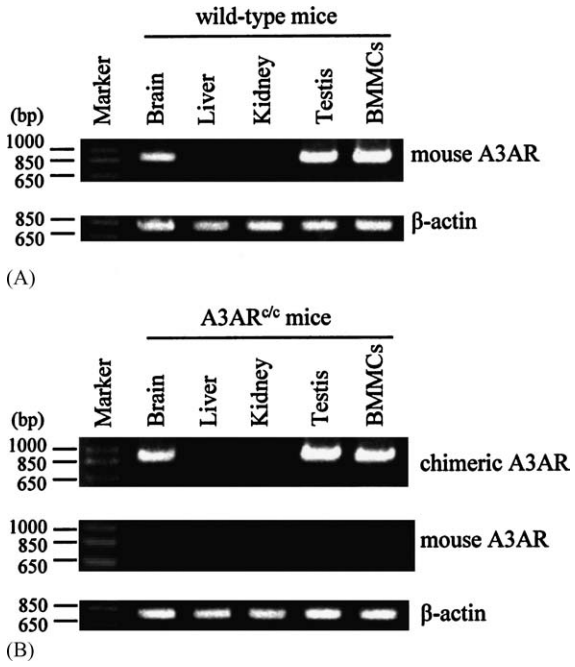

Fig. 4 – Expression of chimeric A3AR mRNA in A3AR$^{c/c}$ mice. The expression levels of mouse or chimeric A3AR mRNA in wild-type (A) and A3AR$^{c/c}$ mice (B) were assayed using RT-PCR. The expression of β-actin mRNA was detected as a control.

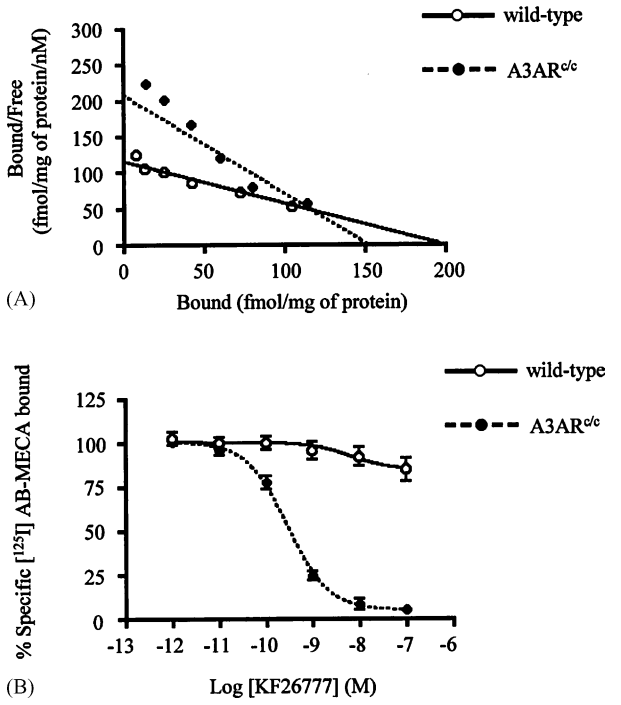

Fig. 5 – Functional expression of chimeric A3AR in BMMCs from A3AR$^{c/c}$ mice. (A) Scatchard plot for the binding of [^{125}I]AB-MECA. The K_d values were 1.71 ± 0.09 nM (wild-type mice, open circles) and 0.73 ± 0.14 nM (A3AR$^{c/c}$ mice, closed circles). The B_{max} values were 194.9 ± 5.6 and 150.3 ± 12.1 fmol/mg of protein (wild-type and A3AR$^{c/c}$ mice, respectively). (B) Competition by KF26777 for the binding of [^{125}I]AB-MECA (0.8 nM). The K_i values were >10,000 nM (wild-type mice, open circles) and 0.15 ± 0.11 nM (A3AR$^{c/c}$ mice, closed circles). Values are the means ± S.D. of three experiments.

3.2. *Normal expression of chimeric A3AR mRNA in A3AR$^{c/c}$ mice*

We measured the mRNA expression levels of chimeric A3AR in A3AR$^{c/c}$ mice by RT-PCR analysis. The expression levels and distribution of the chimeric A3AR mRNA in A3AR$^{c/c}$ mice were the same as those of the mouse A3AR mRNA in wild-type mice, and expression of the mouse A3AR mRNA in A3AR$^{c/c}$ mice was not detected (Fig. 4).

3.3. *Characteristics of [^{125}I]AB-MECA binding in BMMC membranes from A3AR$^{c/c}$ mice*

In order to evaluate whether or not the chimeric A3AR was functionally expressed on mouse BMMCs, the specific binding of the A3AR agonist [^{125}I]AB-MECA was measured using the BMMC membranes (Fig. 5A). The chimeric A3AR on BMMCs from A3AR$^{c/c}$ mice was expressed at the same level as the mouse A3AR on BMMCs from wild-type mice (the B_{max} values for BMMCs from wild-type and A3AR$^{c/c}$ mice were 194.9 ± 5.6 and 150.3 ± 12.1 fmol/mg of protein, respectively). On BMMCs from wild-type mice, the K_d value of [^{125}I]AB-MECA and the K_i value of KF26777, a highly potent and selective antagonist for the human A3AR, were 1.71 ± 0.09 nM and over 10,000 nM, respectively. These values are at the same level as those for the rat A3AR [30,33]. Compared with the low affinity of [^{125}I]AB-MECA for the human A3AR on BMMCs from A3AR$^{h/h}$ mice, in which some of the mouse $G_{i/o}$ proteins were probably uncoupled with the human A3AR [29], the K_d value of [^{125}I]AB-MECA for the chimeric A3AR on BMMCs from A3AR$^{c/c}$ mice was a much higher 0.73 ± 0.14 nM (Fig. 5A), which was equivalent to that for the human A3AR on human cells (0.67 nM [30]). Moreover, the K_i value of KF26777 for the chimeric A3AR on the BMMCs was 0.15 ± 0.11 nM (Fig. 5B), which was also equivalent to that for the human A3AR on human cells (0.20 nM [30]).

3.4. *The chimeric A3AR leads to the mobilization of [Ca^{2+}]$_i$ in BMMCs from A3AR$^{c/c}$ mice*

In order to evaluate whether or not the chimeric A3AR functions normally in mice, we measured the mobilization of [Ca^{2+}]$_i$ induced by the A3AR agonist Cl-IB-MECA in BMMCs from A3AR$^{c/c}$ mice using the fluorescent Ca^{2+} indicator Fluo-3 AM. The increase of [Ca^{2+}]$_i$ in BMMCs from both wild-type and A3AR$^{c/c}$ mice was rapidly induced by Cl-IB-MECA, and the mobilization of [Ca^{2+}]$_i$ in the BMMCs from A3AR$^{c/c}$ mice, but not in those from wild-type mice, was completely antagonized by KF26777 (Fig. 6). These [Ca^{2+}]$_i$ increases, which were induced in a dose-dependent manner with a saturated response of at 100 nM Cl-IB-MECA, were inhibited by the pre-treatment of 200 ng/ml pertussis toxin, an inhibitor of $G_{i/o}$ proteins (data not shown). Similar results were also observed with the fluorescence indicator Fura-2.

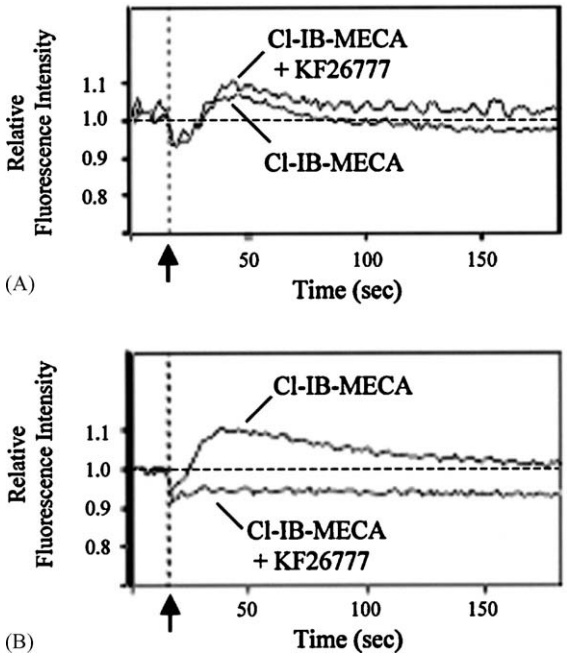

Fig. 6 – The A3AR agonist induces a $[Ca^{2+}]_i$ increase in the BMMCs from A3AR$^{c/c}$ mice. BMMCs derived from wild-type (A) and A3AR$^{c/c}$ mice (B) were preloaded with Fluo-3 AM and then were stimulated with 100 nM Cl-IB-MECA in the absence or presence of 100 nM KF26777. Fluo-3 fluorescence images were registered using an FDSS 6000 system, and the relative fluorescence intensities were plotted.

3.5. *The chimeric A3AR leads to the activation of the PI3Kγ-signaling pathway in BMMCs from A3AR$^{c/c}$ mice*

We previously reported that the human A3AR did not lead to the phosphorylation of ERK1/2 and PKB or the A3AR internalization via PI3Kγ in A3AR$^{h/h}$ mice [29]. To determine whether or not the chimeric A3AR can activate the PI3Kγ-dependent signaling pathway in A3AR$^{c/c}$ mice, we first measured the phosphorylation of ERK1/2 and PKB induced by the chimeric A3AR. The Cl-IB-MECA-stimulated chimeric A3AR led to the phosphorylation of ERK1/2 and PKB in A3AR$^{c/c}$ mice, as it did in wild-type mice (Fig. 7A). Cl-IB-MECA (1, 10, and 100 nM) thus induced the phosphorylation of ERK1/2 and PKB in BMMCs from wild-type and A3AR$^{c/c}$ mice in a dose-dependent manner (Fig. 7B). Next, we examined the rate of chimeric A3AR internalization on the BMMCs induced by Cl-IB-MECA. The changing rate of the chimeric A3AR surface density after treatment of the BMMCs from A3AR$^{c/c}$ mice with Cl-IB-MECA was also equivalent to that from wild-type mice (Fig. 7C).

3.6. *The IgE/antigen-dependent degranulation in BMMCs from A3AR$^{c/c}$ mice is potentiated by the A3AR agonist and completely inhibited by the human A3AR antagonist*

To investigate whether or not the chimeric A3AR can potentiate the mast cell degranulation, the amounts of β-hexosaminidase released from the IgE/antigen-stimulated BMMCs from wild-type, A3AR$^{h/h}$, or A3AR$^{c/c}$ mice potentiated by Cl-IB-MECA were measured as the β-hexosaminidase activity in the supernatants. No differences in the amounts of total β-hexosaminidase in BMMCs from all mice were observed (data not shown). In contrast to BMMCs from A3AR$^{h/h}$ mice (Fig. 8B), Cl-IB-MACA caused a dose-dependent increase in β-hexosaminidase release from BMMCs from both wild-type (Fig. 8A) and A3AR$^{c/c}$ mice (Fig. 8C). The Cl-IB-MECA-induced enhancement of the potentiation of mast cell degranulation in BMMCs from A3AR$^{c/c}$ mice was perfectly antagonized by KF26777 (Fig. 9C), whereas those in BMMCs from wild-type and A3AR$^{h/h}$ mice were unaffected by KF26777 (Fig. 9A and B).

4. Discussion

Previously, we generated A3AR-humanized mice in which the mouse A3AR gene was replaced by the human A3AR cDNA sequence in order to evaluate in vivo pharmacological effects of the highly potent and selective antagonists for the human A3AR [29]. However, the human A3AR was unable to lead to the potentiation of IgE/antigen-dependent mast cell degranulation, even though the human A3AR-induced $[Ca^{2+}]_i$ mobilization was normal. This was thought to be due to the uncoupling of mouse G protein(s) of the $G_{i/o}$ family for the activation of PI3Kγ-dependent signal pathway, but not for the $[Ca^{2+}]_i$ mobilization, to the human A3AR, suggesting that different G proteins of $G_{i/o}$ family stimulate these pathways downstream of A3AR. Therefore, we generated A3AR functionally humanized mice, in which the A3AR gene was replaced with a human/mouse chimeric A3AR sequence consisting of the intracellular loop regions from the mouse A3AR as G protein-coupled regions and the extracellular loop and intramembrane regions from the human A3AR as agonist- and antagonist-binding regions (Fig. 2). The homologous recombination method was employed according to the strategy shown in Fig. 3A.

Many GPCRs, such as 5-hydroxytryptamine 1B ($5HT_{1B}$) receptor, neurokinin-1 (NK-1) receptor, muscarinic M2 receptor, α2-adrenergic receptor, β2-adrenergic receptor, cholecystokinin-B receptor, neurotensin receptor, and prostaglandin D2 receptor, are known to have different binding affinities for agonists and/or antagonists for the human and non-human receptors due to the low interspecies homologies [5]. Some human/non-human chimeric studies have been carried out to investigate the mechanism of these interspecies differences. Human/rodent chimeric studies of GPCRs $5HT_{1B}$ and NK-1 receptors have made it clear that species differences in the antagonist-binding affinities between humans and rodents are due to the amino acid residue in the 7th intramembrane region of these receptors [34–36]. In the α2-adrenergic receptor, the species difference in antagonist-binding affinity between humans and rodents is shown to be due to the amino acid residue in the 5th intramembrane region [37]. Studies of the human/frog or mouse chimeric gonadotropin-releasing hormone receptor (GnRHR) show that the 2nd extracellular loop region of the GnRHR is essential for ligand binding [38,39]. Although there have been no previous studies on chimeric A3AR of humans and other species, site-directed mutagenesis analyses of amino acid residues within the human A3AR have

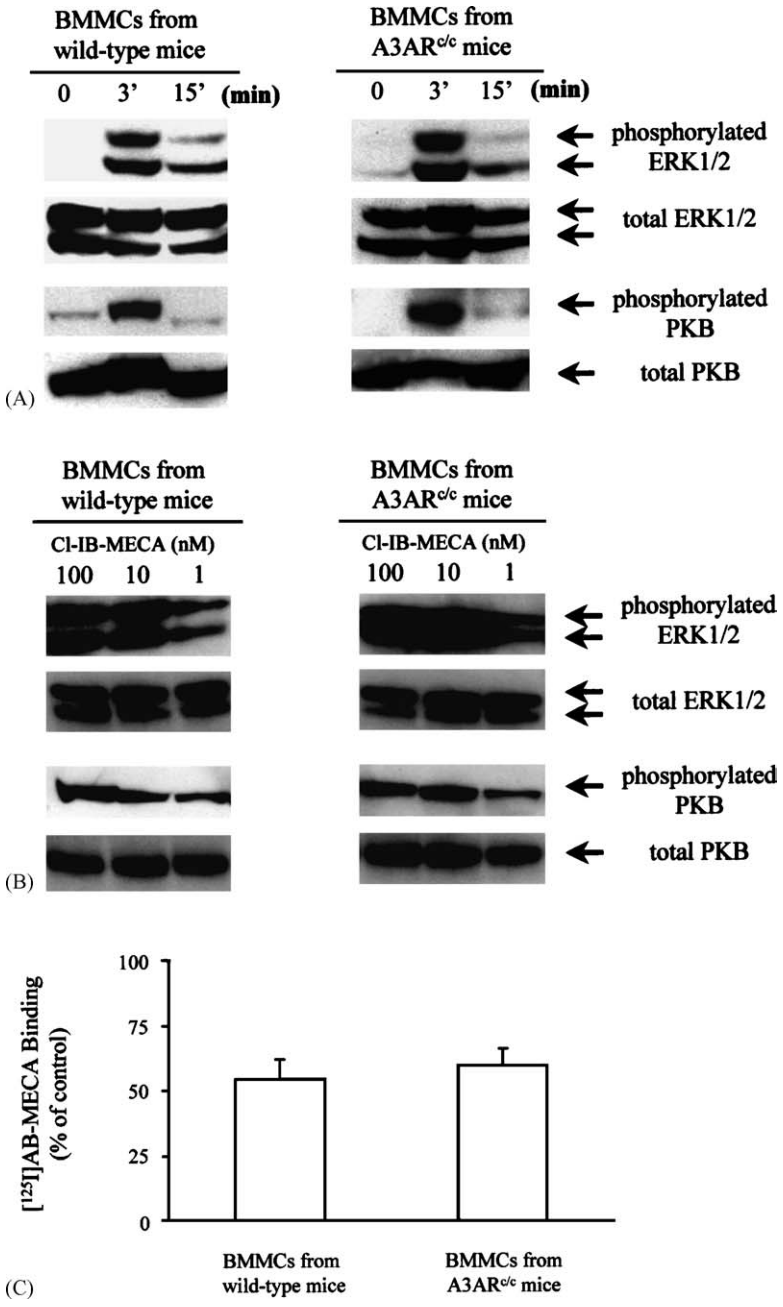

Fig. 7 – The A3AR agonist leads to the phosphorylation of ERK1/2 and PKB and the A3AR internalization in BMMCs from A3AR$^{c/c}$ mice. (A) The phosphorylation of ERK1/2 and PKB by Cl-IB-MECA. BMMCs from wild-type (left panels) and A3AR$^{c/c}$ mice (right panels) were stimulated by 1 μM Cl-IB-MECA for 0, 3, and 15 min. The phosphorylation of ERK1/2 and PKB was detected by Western blot analysis with anti-phosphorylated ERK1/2 and PKB antibodies. Total ERK1/2 and PKB levels were detected with anti-ERK1/2 and anti-PKB antibodies. (B) The concentration-dependent phosphorylation of ERK1/2 and PKB by Cl-IB-MECA in BMMCs from wild-type (left panels) and A3AR$^{c/c}$ mice (right panels) treated with the indicated concentration of Cl-IB-NECA for 3 min. (C) The A3AR internalization induced by Cl-IB-MECA. BMMCs were incubated with 1 μM Cl-IB-MECA at 37 °C for 15 min. After incubation, the A3AR density on the cell surface was evaluated by measuring the extent of [^{125}I]AB-MECA binding for 120 min. Data were expressed as a percentage of total binding versus control Cl-IB-MECA-untreated cells (100%). Values are the means ± S.E.M. of five different experiments.

demonstrated that several amino acid residues in the extracellular and intramembrane regions are critical for the antagonist-binding affinity [40–43]. All of these studies were focused on either the extracellular or intramembrane regions, despite the fact that the intracellular regions of GPCRs are well known to be critical for intracellular signaling. Thus, we decided to substitute whole intracellular loop sequences in the human A3AR for the corresponding sequences of the mouse

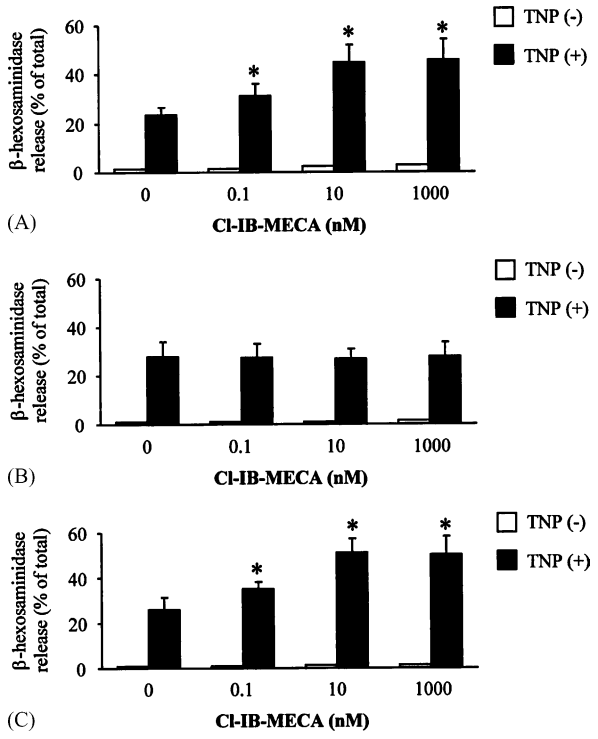

Fig. 8 – The A3AR agonist potentiates IgE/antigen-dependent mast cell degranulation in BMMCs from A3AR$^{c/c}$ mice. BMMCs derived from wild-type (A), A3AR$^{h/h}$ (B), and A3AR$^{c/c}$ mice (C) were pre-incubated overnight with anti-TNP IgE and then were incubated in the absence (open bars) or presence (closed bars) of antigen, 10 ng/ml TNP-BSA, for 20 min. The cells were incubated with Cl-IB-MECA (0, 0.1, 10, and 1000 nM) for 1 min prior to stimulation with the antigen. β-Hexosaminidase released in the supernatant was measured using *p*-nitrophenyl *N*-acetyl-β-glucosaminide. Values are the means ± S.E.M. of five different experiments. $^{*}p < 0.05$ compared with the values in the absence of Cl-IB-MECA.

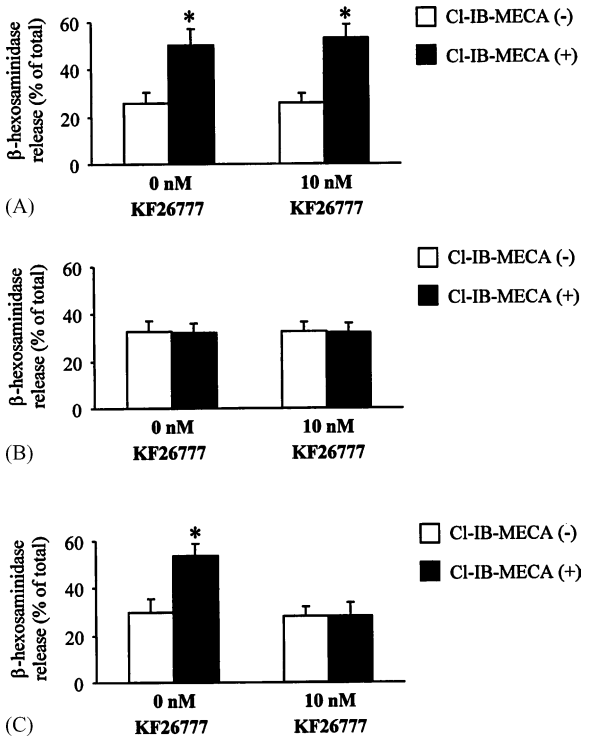

Fig. 9 – The potentiation of mast cell degranulation in BMMCs from A3AR$^{c/c}$ mice was completely antagonized by the human A3AR antagonist KF26777. BMMCs from wild-type (A), A3AR$^{h/h}$ (B), and A3AR$^{c/c}$ mice (C) were pre-incubated overnight with anti-TNP IgE and were incubated with 0 or 10 nM KF26777 for 1 min. The cells were incubated in absence (open bars) or presence (closed bars) of 10 nM Cl-IB-MECA for 1 min prior to stimulation with 10 ng/ml TNP-BSA. After stimulation for 20 min, β-hexosaminidase released in the supernatant was measured using *p*-nitrophenyl *N*-acetyl-β-glucosaminide. Values are the means ± S.E.M. of five different experiments. $^{*}p < 0.05$ compared with the values in the absence of Cl-IB-MECA.

A3AR to determine whether interspecies differences exist in the mechanism of G protein/GPCR coupling.

We first examined the expression of the human/mouse chimeric A3AR in A3AR$^{c/c}$ mice we generated. The expression levels of the chimeric A3AR in A3AR$^{c/c}$ mice were equal to those of the mouse A3AR in wild-type mice (Figs. 4 and 5). Next, we evaluated whether or not the chimeric A3AR would lead to the physiological responses in A3AR$^{c/c}$ mice. The agonist-mediated chimeric A3AR elevated the $[Ca^{2+}]_i$ in BMMCs from A3AR$^{c/c}$ mice, and this elevation was completely antagonized by KF26777, the human A3AR-specific antagonist (Fig. 6). Moreover, as expected, like the human A3AR in human cells, the agonist-stimulated chimeric A3AR led to the phosphorylation of ERK1/2 and PKB (Fig. 7A and B), followed by the potentiation of IgE/antigen-dependent mast cell degranulation (Fig. 8) and the A3AR internalization (Fig. 7C) in BMMCs from A3AR$^{c/c}$ mice, all of which activities are lacking in the A3AR$^{h/h}$ mice. These results clearly demonstrate that the human/mouse chimeric A3AR is able to activate PI3Kγ through some of the mouse G protein couplings that are involved in the potentiation of mast cell degranulation in mice. In addition, the potentiation was completely antagonized by KF26777, which is never observed in wild-type mice (Fig. 9). These results demonstrate that the A3AR$^{c/c}$ mice have potential as A3AR functionally humanized mice, which is the first rodent model for the pharmacological evaluation of human A3AR antagonists. More detailed analysis of the chimeric A3AR using the human A3AR antagonist in BMMCs and other A3AR highly expressing tissues such as brain and testis will help to further clarify the physiological function of A3AR.

It is commonly assumed that the uncoupling of a G protein form GPCR leads to a relative reduction in the binding affinity of the ligand to the GPCR [44]. Actually, low binding affinities of the A3AR agonist to the human and canine A3AR in the transgenic mice have been observed [29,45]. The binding affinity of A3AR agonist [^{125}I]AB-MECA to the human A3AR on BMMCs from A3AR$^{h/h}$ mice was 1.42 nM, which is two-fold lower than that on human cell lines (the K_d value for the

human A3AR on the human cell line is 0.67 ± 0.03 nM [30]) [29]. In A3AR$^{c/c}$ mice, the K_d value of [^{125}I]AB-MECA to the human/mouse chimeric A3AR on the BMMCs was 0.73 ± 0.14 nM, equivalent to the human A3AR in human cells (Fig. 5A). Taken together, the findings that chimeric A3AR activated the PI3Kγ-dependent signaling pathway, and that the A3AR agonist in A3AR$^{c/c}$ mice has the same binding affinity as the human A3AR suggest that some of the mouse G proteins that can not be coupled to the human A3AR can be coupled to the chimeric A3AR. Our findings provide the first direct evidence that the uncoupling of mouse G protein(s) to the human A3AR is due to the sequence difference in the intracellular regions of A3AR between humans and mice.

In general, signaling pathways of many human GPCRs, including A3AR, are investigated using human receptor-over-expressing cells derived from different species, such as Chinese hamster ovary cell line. The results of these studies may reflect interspecies differences, and if so, then these differences must be taken into consideration to understand the native physiological response in vivo. Studies on bovine rhodopsin, for which the three-dimensional structure has been reported, indicate that the contact surfaces for G protein-binding to GPCR include all intracellular regions of the GPCR [46]. On the other hand, each intracellular region of A3AR has different interspecies homology between humans and rodents, and the homology of the 4th intracellular region is much lower than that of other intracellular regions (the 1st, 2nd, 3rd, and 4th intracellular region homologies are 80, 85, 84, and 62%, respectively). Identification of the intracellular region(s) for the coupling of G protein(s) is an interesting issue and still remains to be solved.

In summary, we here succeeded in generating A3AR functionally humanized mice by replacing the mouse A3AR gene with the human/mouse chimeric A3AR, in which whole intracellular regions of the human A3AR were substituted for the corresponding regions of the mouse A3AR. The A3AR functionally humanized mice can be widely employed for the pharmacological evaluation of human A3AR antagonists and further elucidation of the in vivo physiological roles of A3AR. Our finding is the first direct evidence of the uncoupling of mouse G protein(s) to the human GPCR A3AR, which should provide new insight into the mechanism of G protein/GPCR coupling and its differences among species.

Acknowledgements

We thank Drs. Katsutoshi Sasaki, Kazumi Kurata-Miura, and Satoshi Saeki for helpful discussion.

REFERENCES

[1] Stadel JM, Wilson S, Bergsma DJ, Orphan G. protein-coupled receptors: a neglected opportunity for pioneer drug discovery. Trends Pharmacol Sci 1997;18:430–7.
[2] Rohrer DK, Kobilka BK. G protein-coupled receptors: functional and mechanistic insights through altered gene expression. Physiol Rev 1998;78:35–52.
[3] Flower DR. Modelling G-protein-coupled receptors for drug design. Biochim Biophys Acta 1999;1422:207–34.
[4] Marinissen MJ, Gutkind JS. G-protein-coupled receptors and signaling networks: emerging paradigms. Trends Pharmacol Sci 2001;22:368–76.
[5] Watson S, Arkinstall S. The G-protein linked receptor FactsBook. London: Academic Press, 1994.
[6] Baraldi PG, Cacciari B, Romagnoli R, Merighi S, Varani K, Borea PA, et al. A_3 adenosine receptor ligands: history and perspectives. Med Res Rev 2000;20:103–28.
[7] Müller CE. Medicinal chemistry of adenosine A_3 receptor ligands. Curr Top Med Chem 2003;3:445–62.
[8] Olah ME, Stiles GL. Adenosine receptor subtypes: characterization and therapeutic regulation. Annu Rev Pharmacol Toxicol 1995;35:581–606.
[9] Fredholm BB, IJzerman AP, Jacobson KA, Klotz KN, Linden J. International Union of Pharmacology. XXV. Nomenclature and classification of adenosine receptors. Pharmacol Rev 2001;53:527–52.
[10] Klinger M, Freissmuth M, Nanoff C. Adenosine receptors: G protein-mediated signaling and the role of accessory proteins. Cell Signal 2002;14:99–108.
[11] Schulte G, Fredholm BB. Signaling from adenosine receptors to mitogen-activated protein kinases. Cell Signal 2003;15:813–27.
[12] Wymann MP, Bjorklof K, Calvez R, Finan P, Thomast M, Trifilieff A, et al. Phosphoinositide 3-kinase γ: a key modulator in inflammation and allergy. Biochem Soc Trans 2003;31:275–80.
[13] Hammarberg C, Fredholm BB, Schulte G. Adenosine A_3 receptor-mediated regulation of p38 and extracellular-regulated kinase ERK1/2 via phosphatidylinositol-3′-kinase. Biochem Pharmacol 2004;67:129–34.
[14] Laffargue M, Calvez R, Finan P, Trifilieff A, Barbier M, Altruda F, et al. Phosphoinositide 3-kinase γ is an essential amplifier of mast cell function. Immunity 2002;16:441–51.
[15] Trincavelli ML, Tuscano D, Marroni M, Klotz KN, Lucacchini A, Martini C. Involvement of mitogen protein kinase cascade in agonist-mediated human A_3 adenosine receptor regulation. Biochim Biophys Acta 2002;1591:55–62.
[16] Fishman P, Bar-Yehuda S. Pharmacology and therapeutic applications of A_3 receptor subtype. Curr Top Med Chem 2003;3:463–9.
[17] Brambilla R, Cattabeni F, Ceruti S, Barbieri D, Franceschi C, Kim YC, et al. Activation of the A_3 adenosine receptor affects cell cycle progression and cell growth. Naunyn Schmiedebergs Arch Pharmacol 2000;361:225–34.
[18] Gao Z, Li BS, Day YJ, Linden J. A_3 adenosine receptor activation triggers phosphorylation of protein kinase B and protects rat basophilic leukemia 2H3 mast cells from apoptosis. Mol Pharmacol 2001;59:76–82.
[19] Merighi S, Benini A, Mirandola P, Gessi S, Varani K, Leung E, et al. A_3 adenosine receptor activation inhibits cell proliferation via phosphatidylinositol 3-kinase/Akt-dependent inhibition of the extracellular signal-regulated kinase 1/2 phosphorylation in A375 human melanoma cells. J Biol Chem 2005;280:19516–2.
[20] Ramkumar V, Stiles GL, Beaven MA, Ali H. The A_3 adenosine receptor is the unique adenosine receptor, which facilitates release of allergic mediators in mast cells. J Biol Chem 1993;268:16887–90.
[21] Salvatore CA, Tilley SL, Latour AM, Fletcher DS, Koller BH, Jacobson MA. Disruption of the A_3 adenosine receptor gene in mice and its effect on stimulated inflammatory cells. J Biol Chem 2000;275:4429–34.
[22] Tilley SL, Tsai M, Williams CM, Wang ZS, Erikson CJ, Galli SJ, et al. Identification of A_3 receptor and mast cell-dependent and -independent components of adenosine-mediated airway responsiveness in mice. J Immunol 2003;171:331–7.

[23] Zhong H, Shlykov SG, Molina JG, Sanborn BM, Jacobson MA, Tilley SL, et al. Activation of murine lung mast cells by the adenosine A_3 receptor. J Immunol 2003;171:338–45.
[24] Feoktistov I, Ryzhov S, Goldstein AE, Biaggioni I. Mast cell-mediated stimulation of angiogenesis: cooperative interaction between A_{2B} and A_3 adenosine receptors. Circ Res 2003;92:485–92.
[25] Kohno Y, Ji X, Mawhorter SD, Koshiba M, Jacobson KA. Activation of A_3 adenosine receptors on human eosinophils elevates intracellular calcium. Blood 1996;88:3569–74.
[26] Young HW, Molina JG, Dimina D, Zhong H, Jacobson M, Chan LN, et al. A_3 adenosine receptor signaling contributes to airway inflammation and mucus production in adenosine deaminase-deficient mice. J Immunol 2004;173:1380–9.
[27] Gessi S, Varani K, Merighi S, Cattabriga E, Iannotta V, Leung E, et al. A_3 adenosine receptors in human neutrophils and promyelocytic HL60 cells: a pharmacological and biochemical study. Mol Pharmacol 2002;61:415–24.
[28] Harish A, Hohana G, Fishman P, Arnon O, Bar-Yehuda S. A_3 adenosine receptor agonist potentiates natural killer cell activity. Int J Oncol 2003;23:1245–9.
[29] Yamano K, Inoue M, Masaki S, Saki M, Ichimura M, Satoh M. Human adenosine A3 receptor leads to intracellular Ca^{2+} mobilization but is insufficient to activate the signaling pathway via phosphoinositide 3-kinase γ in mice. Biochem Pharmacol 2005;70:1487–96.
[30] Saki M, Tsumuki H, Nonaka H, Shimada J, Ichimura M. KF26777 (2-(4-bromophenyl)-7,8-dihydro-4-propyl-1*H*-imidazo[2,1-i]purin-5(4*H*)-one dihydrochloride), a new potent and selective adenosine A_3 receptor antagonist. Eur J Pharmacol 2002;444:133–41.
[31] Nakamura K, Tanaka Y, Fujino I, Hirayama N, Shitara K, Hanai N. Dissection and optimization of immune effector functions of humanized anti-ganglioside GM2 monoclonal antibody. Mol Immunol 2002;37:1035–46.
[32] Cheng Y, Prusoff WH. Relationship between the inhibition constant (K_i) and the concentration of inhibitor, which causes 50% inhibition (IC_{50}) of an enzymatic reaction. Biochem Pharmacol 1973;22:3099–108.
[33] Li AH, Moro S, Forsyth N, Melman N, Ji XD, Jacobson KA. Synthesis, CoMFA analysis, and receptor docking of 3,5-diacyl-2,4-dialkylpyridine derivatives as selective A_3 adenosine receptor antagonists. J Med Chem 1999; 42:706–21.
[34] Oksenberg D, Marsters SA, O'Dowd BF, Jin H, Havlik S, Peroutka SJ, et al. A single amino-acid difference confers major pharmacological variation between human and rodent 5-HT_{1B} receptors. Nature 1992;360:161–3.
[35] Fong TM, Yu H, Strader CD. Molecular basis for the species selectivity of the neurokinin-1 receptor antagonists CP-96,345 and RP67580. J Biol Chem 1992;267:25668–71.
[36] Sachais BS, Snider RM, Lowe III JA, Krause JE. Molecular basis for the species selectivity of the substance P antagonist CP-96,345. J Biol Chem 1993;268:2319–23.
[37] Link R, Daunt D, Barsh G, Chruscinski A, Kobilka B. Cloning of two mouse genes encoding α2-adrenergic receptor subtypes and identification of a single amino acid in the mouse α2-C10 homolog responsible for an interspecies variation in antagonist binding. Mol Pharmacol 1992; 42:16–27.
[38] Arora KK, Chung HO, Catt KJ. Influence of a species-specific extracellular amino acid on expression and function of the human gonadotropin-releasing hormone receptor. Mol Endocrinol 1999;13:890–6.
[39] Ott TR, Troskie BE, Roeske RW, Illing N, Flanagan CA, Millar RP. Two mutations in extracellular loop 2 of the human GnRH receptor convert an antagonist to an agonist. Mol Endocrinol 2002;16:1079–88.
[40] Jacobson KA, Gao ZG, Chen A, Barak D, Kim SA, Lee K, et al. Neoceptor concept based on molecular complementarity in GPCRs: a mutant adenosine A_3 receptor with selectively enhanced affinity for amine-modified nucleosides. J Med Chem 2001;44:4125–36.
[41] Gao ZG, Chen A, Barak D, Kim SK, Müller CE, Jacobson KA. Identification by site-directed mutagenesis of residues involved in ligand recognition and activation of the human A_3 adenosine receptor. J Biol Chem 2002;277: 19056–63.
[42] Gao ZG, Kim SK, Biadatti T, Chen W, Lee K, Barak D, et al. Structural determinants of A_3 adenosine receptor activation: nucleoside ligands at the agonist/antagonist boundary. J Med Chem 2002;45:4471–84.
[43] Gao ZG, Kim SK, Gross AS, Chen A, Blaustein JB, Jacobson KA. Identification of essential residues involved in the allosteric modulation of the human A_3 adenosine receptor. Mol Pharmacol 2003;63:1021–31.
[44] Christopoulos A, Kenakin T. G protein-coupled receptor allosterism and complexing. Pharmacol Rev 2002; 54:323–74.
[45] Black Jr RG, Guo Y, Ge ZD, Murphree SS, Prabhu SD, Jones WK, et al. Gene dosage-dependent effects of cardiac-specific overexpression of the A_3 adenosine receptor. Circ Res 2002;91:165–72.
[46] Yeagle PL, Albert AD. A conformational trigger for activation of a G protein by a G protein-coupled receptor. Biochemistry 2003;42:1365–8.